The Combined activities of FtsW and MurJ are required for lipid II translocation during cell division in *Escherichia coli*

Xiaolong Liu[1], Nils Y. Meiresonne[1], Ahmed Bouhss[2,3] and Tanneke den Blaauwen[1*]

[1]*Bacterial Cell Biology, Swammerdam Institute for Life Sciences, Faculty of Science, University of Amsterdam, Amsterdam, The Netherlands*

[2]*Institute for Integrative Biology of the Cell (I2BC), CEA, CNRS, Univ Paris-Sud, Université Paris-Saclay, 91198, Gif-sur-Yvette, France.*

[3]*Laboratoire Structure-Activité des Biomolécules Normales et Pathologiques (SABNP), Univ Evry, INSERM U1204, Université Paris-Saclay, 91025 Evry, France*

*Corresponding author

Abstract

Peptidoglycan (PG) is the unique cell shape-determining component of the bacterial envelope, and is a key target for antibiotics. PG synthesis requires the transmembrane movement of the precursor lipid II by its flippase. Evidence has been shown that the inner membrane protein MurJ is able to provide this activity in *E. coli*. However, how MurJ functions has thus far not been reported. Here, by using functional fluorescent MurJ fusion proteins, we show *in vivo* that MurJ localizes both in the lateral membrane and at midcell, and is recruited to midcell simultaneously with late-localizing divisome proteins and the proteins MraY and MurG, which are required for Lipid II synthesis. We show that this septal localization of MurJ is dependent on the divisome activation, lipid II synthesis and FtsW activity. Investigations on localization of MurJ cysteine variants whose function can be inactivated by the cysteine-binding molecule MTSES indicate that the inward-facing conformation is the default state for MurJ. The loss-of-function MurJ mutant proteins are in this conformation and can still be recruited, while MTSES traps functional mutants A29C and S263C in the outward-facing conformation that cannot be recruited, and causes loss of localization and function of MurJ. Our results also indicate that the flipping of lipid II coincides with the MurJ conformational change from inward-facing into outward-facing conformation. Combining the available data, a model is deduced in which binding and presenting of lipid II by FtsW recruits MurJ and allows lipid II flipping by MurJ.

Key wards: peptidoglycan synthesis, lipid II, flippase, divisome, conformational changes, *E. coli*

Significance Statement

Biosynthesis of bacterial peptidoglycan requires the flipping of lipid-linked disaccharide-pentapeptide precursor lipid II from the inside to the outside of the cytoplasm membrane by the so-called flippase. To date, the conflicting evidences on the flippase candidates RodA, FtsW and MurJ have prevented the unequivocal identification of the flippase. Here we provide evidence that supports MurJ as the

Lipid-II flippase and FtsW as the provider of lipid II to MurJ reconciling the thus far conflicting data.

Introduction

Rod-shaped bacteria such as the Gram-negative bacterium *Escherichia coli* grow by elongation and binary fission. One of the requirements for proliferation is the enlargement of their cell envelope, which contains an inner membrane (IM) and an outer membrane (OM). The shape of the bacterium is determined by the shape of its peptidoglycan (PG) layer, which is attached to the outer membrane in the periplasmic space located between both membranes of the envelope (1). The PG layer is a mesh-like heteropolymeric macromolecule of alternating *N*-acetylmuramyl-peptides (MurNAc-pentapeptides) and *N*-acetylglucosamine (GlcNAc) disaccharides that are connected by a β-(1,4) bond forming glycan chains that are crosslinked between *meso* diaminopimelic acid (DAP) and D-Ala at the third and fourth position of the acceptor and donor stem peptide, respectively (2). The biosynthesis of PG is a complicated process that can be divided into 3 stages. In the cytoplasmic stage, the nucleotide precursors UDP-GlcNAc and UDP-MurNAc-pentapeptide are synthesized from fructose-6-phosphate by the GlmSMU and MurABCDEF proteins, respectively (3). In the IM stage, the undecaprenyl-pyrophosphate- (C_{55}) linked intermediates lipid I (C_{55}-MurNAc-pentapeptide) and lipid II (C_{55}-MurNAc(-pentapeptide)-GlcNAc) are formed by the MraY and MurG proteins, respectively (2). During this stage, lipid II, containing the disaccharide-peptide moiety, the building unit of peptidoglycan, is translocated by a "flippase" across the IM (3–7). In the periplasmic stage, the MurNAc-pentapeptide-GlcNAc component of lipid II is inserted into the PG layer by the glycosyltransferase and transpeptidase activities of various PBPs (8, 9), and the lipoyl moiety C_{55}-PP is cleaved off and recycled (10).

In *E. coli,* new PG-building units are inserted into the existing PG layer during length growth by a protein complex termed the elongasome, whereas during division new poles are synthesized from completely new material (11) by proteins that collectively have been termed the divisome (12). The elongasome is organized by the actin homolog MreB, which localizes underneath the IM in patches in a helix-like distribution. MreB is bound to the membrane by its amphipathic helix, and interacts

98 with the bitopic membrane protein RodZ, the integral membrane proteins MreD and
99 MreC, and the PG synthesis essential proteins RodA and PBP2 (12–16). How the
100 elongasome is regulated is not yet very clear whereas in contrast, cell division has
101 been well investigated. During cell division, at least 20 proteins are recruited to
102 midcell to form the divisome. The tubulin homologue FtsZ is attached to the IM at
103 midcell by the anchor proteins FtsA and ZipA, and polymerizes to form the Z-ring (17,
104 18). Simultaneously, other proteins, such as the Zap proteins and FtsEX, are recruited
105 to the ring to form the early divisome or protoring. The protoring then recruits the
106 later divisome proteins FtsK, FtsQ, FtsL, FtsB, FtsW, FtsI (PBP3), PBP1B, FtsN (19),
107 and a number of hydrolases and regulatory proteins (20) to form the mature divisome
108 (21). The arrival of FtsN is believed to initiate PG synthesis by elevating the
109 repression of the FtsQLB complex (22–24). The assembled divisome functions as a
110 scaffold to initiate septal PG synthesis, OM constriction, and the cleavage of the PG
111 layer to separate daughter cells (20). Septal PG synthesis is mainly orchestrated by
112 PBP3 and PBP1B (9, 25), but PBP1A can substitute for PBP1B (26, 27). OM
113 constriction is organized by the Tol/Pal system, which forms a complex connecting
114 IM and OM (28, 29). Tightly controlled amidase activity is involved in the separation
115 of the daughter cells (30).
116
117 Although the stages of PG synthesis are well understood, conflicting information on
118 the flipping of lipid II across the IM has been published over the last few years. In *E.*
119 *coli*, RodA and FtsW that belong to the SEDS (shape, elongation, division,
120 sporulation) family, and MurJ that belongs to the MOP (multidrug/oligo-saccharidyl-
121 lipid/polysaccharide) export super family (31), are reported as candidates as lipid II
122 flippase, either functioning in elongation or division only or in both (6, 32, 33). An
123 alternative activity as glycosyltransferase was recently reported for RodA in *Bacillus*
124 *subtilis* (34), while the debate which protein is responsible for lipid II flipping is still
125 going on.
126
127 FtsW is an essential integral membrane cell division protein with 10 trans-membrane
128 helixes (TMHs) and is conserved in most bacterial species that have a PG cell wall
129 (35). FtsW and PBP3 form a complex that is recruited to midcell by the FtsQLB
130 complex (36–38). FtsW was shown *in vitro* to have lipid II binding and flipping
131 activity, for which two charged residues in TMH 4, arginine 145 and lysine 153,

132 appeared to be essential, while no lipid II interaction or flipping activity was detected
133 for MurJ *in vitro* (38–40).
134
135 MurJ is an essential IM protein that contains 14 TMHs with both C- and N-termini in
136 the cytoplasm (41, 42). Earlier functional and structural studies of MurJ reveal an
137 outward-facing central cavity that is formed by TMHs 1, 2, 7 and 8, which contain
138 several charged residues that are essential for MurJ function (41, 42). The observation
139 of an open inward-facing conformation in the crystal structure of MurJ from
140 *Thermosipho africanus* ($MurJ_{TA}$) suggests alternative conformational changes of
141 MurJ (43). *In vivo* evidence favors MurJ over FtsW as the lipid II flippase, and
142 depletion of MurJ causes the accumulation of lipid II (31, 32, 44, 45). Interestingly,
143 the function of MurJ in *E. coli* can be replaced by the flippases WzK, Amj and YtgP
144 from other species that lack sequence identify and similarity between them (46–48).
145 Although published data presents evidence that MurJ is the lipid II flippase, it is still
146 not clear where and how MurJ functions in bacterial cells. In this study, by visualizing
147 the cellular localization of MurJ with functional fluorescent protein fusions, we
148 provided new evidence to support MurJ as the flippase and show how MurJ performs
149 its function during PG synthesis.
150
151
152 **Results**

153 **Fluorescent-protein fusions to the N-terminus of MurJ are functional**. We
154 generated fluorescent protein (FP) fusions to MurJ in *E. coli* and investigated their
155 function and localization in cells. Initially, two low-copy-number plasmids, pTHV037
156 and pSAV057, were used for expression of fused FP-MurJ under control of a down-
157 regulated $P_{trcdown}$ promoter to avoid high overexpression (49). Based on the physical
158 properties of fluorescent proteins (50, 51), green fluorescent protein mNeonGreen
159 (mNG) and red fluorescent protein mCherry (mCh) were chosen for MurJ fusions.
160 Fusions were tested for their ability to complement a MurJ-depletion strain (Material
161 and Methods).
162
163 FP fusions to either the N-terminus or the C-terminus of MurJ with different linkers
164 of Gly-Gly-Ser (GGS) repeats (52) were constructed. The N-terminal MurJ fusions

165 were fully functional in the absence of MurJ and localized to the IM, while C-terminal
166 fusions were less functional or not functional at all (Table 1). Among these, the N-
167 terminal mNG fusion with a $(GGS)_2$ linker showed the most stable and strongest
168 fluorescence signals, while for mCh, the fusion without linker was better, and thus
169 they were chosen for further studies. The crystal structure of MurJ from *T. africanus*
170 reveals that TMHs 13 and 14 form a hydrophobic groove, which penetrates into the
171 central transport cavity and is hypothesized to be important for lipid II binding (43).
172 The loss of function of MurJ C-terminal fusions might be caused by defects in folding
173 and groove formation.
174
175 **MurJ localizes in the lateral wall and also at midcell**. MurJ is reported to be
176 present at 674 and 78 molecules per cell when grown in rich and minimal medium,
177 respectively (53). In order to characterize MurJ at its endogenous expression level, the
178 MurJ fusion was introduced into the *E. coli* chromosome at its native locus. The
179 existence of the native promoter p_{murJ} was confirmed by inserting a divergently
180 transcribed chloramphenicol cassette between the stop codon of gene *yceM* upstream
181 of *murJ* and the putative *murJ* promoter (Fig. S1A). However, attempts to introduce
182 FP-fused MurJ under the native *murJ* promoter failed, apart from a mCh fusion,
183 which yielded a strain with defects in cell morphology and growth (Fig. S1B). Since
184 the plasmid expressed fusions were fully functional, a likely explanation for the
185 morphological defect could be that the decreased expression of the fusion under the
186 native *murJ* promoter is not enough to support growth. Therefore, we replaced the
187 chromosomal *murJ* gene with *fp-murJ* constructs transcribed under the control of
188 $p_{trcdown}$ promoter to generate strains XL08 and XL09 (Material and Methods). No
189 defects on growth or morphology were observed (Fig. S1 C and D). Strain XL08 was
190 grown to steady state in minimal glucose medium (Gb1) at 28°C to be able to
191 correlate its length to its cell division cycle age (18, 54), and the localization of MurJ
192 in living *E. coli* cells was analyzed using ImageJ and the Coli-Inspector of ObjectJ
193 (54). The mass double time (MD) of this strain is 83 minutes, which is close to 80
194 minutes of wild-type *E. coli* (54). MurJ localized in the cylindrical part of the cells as
195 well as specifically at midcell in dividing cells (Fig. 1). After normalizing and plotting
196 the fluorescence profiles into 10 age groups, a clear midcell localization was observed
197 starting from 50%-60% of the cell cycle. To show that this accumulation was not an
198 effect of double membrane formation during cell invagination, the localization of

199 mNG-$(GGS)_2$-GlpT was introduced as control. GlpT (glycerol-3-phosphate
200 transporter) is the major transporter for the uptake of *sn*-glycerol 3-phosphate in *E.*
201 *coli*. It was reported to have 12 TMHs and to function as monomer (55), which
202 diffuses homogenously in the IM (56). It was therefore expected to show homogenous
203 membrane localization. Like for MurJ, the localization of mNG-$(GGS)_2$-GlpT was
204 imaged and analyzed. As expected, GlpT localized homogenously in the membrane
205 without midcell accumulation (Fig. 1B). After plotting into 10 age groups, GlpT
206 showed a clear difference with MurJ, and no enhanced fluorescence was observed at
207 midcell during constriction (Fig. 1A). The differences between the localization
208 patterns of the two proteins are also obvious in images of the cells (Fig. 1C). The
209 specific localization pattern of MurJ suggests that MurJ is likely involved in both
210 length growth and cell division.
211
212 **MurJ is recruited to midcell simultaneously with the PG synthesis proteins.**
213 Since potential changes in MurJ cylindrical localization is not easily visualized, we
214 focused on the MurJ septal localization. The midcell localization of MurJ promoted us
215 to investigate at which cell division cycle age it was recruited. Because XL08 is not a
216 wild-type strain, we could not directly compare the timing of localization of MurJ
217 with data from the literature (70). Therefore, the timing of localization of MurJ, the
218 early and late localizing proteins FtsZ and FtsN, respectively, and the proteins MraY
219 and MurG, which synthesize Lipid I and lipid II, respectively (21, 23, 57–60) was
220 determined in steady-state grown strain XL08. Cells from the same culture and optical
221 density were either imaged live for MurJ localization or were fixed with FAGA (2.8%
222 formaldehyde and 0.04% glutaraldehyde) and subsequently immunolabeled with
223 antibodies specific for the above mentioned proteins (61). As shown in Fig 2, the
224 early divisome protein FtsZ was recruited at midcell at about 25% of cell cycle, and
225 the core divisome assembly completed by the midcell arrival of FtsN at 40% of cell
226 cycle. Interestingly, MraY, MurG and MurJ accumulated at midcell simultaneously
227 between 40%-50% of cell cycle at the later stage of divisome assembly. These results
228 indicate that MurJ is very likely functioning together with the PG synthesis complex,
229 which would be in agreement with its function as a lipid II flippase.
230
231 **MurJ requires a mature divisome for midcell localization**. The timing of MurJ
232 midcell localization raised the question whether its localization is dependent on

233 particular divisome proteins. To answer this, the mNG-$(GGS)_2$-MurJ chromosomal
234 fusion was introduced into a series of temperature-sensitive cell division mutant
235 strains. First was established that MurJ still localized at midcell in a wild-type
236 background at the restrictive temperature (Fig. 3A). FtsA is an essential early
237 divisome protein that anchors the Z-ring to the IM (62, 63). The absence of FtsA
238 causes filamentous growth of *E. coli*, as the downstream divisome proteins are not
239 recruited to midcell (64). In the FtsA(*Ts*) background, MurJ showed normal midcell
240 localization when grown at permissive temperature. However, when grown at 42 °C
241 MurJ midcell localization was lost, and MurJ only localized in the filamentous
242 cylindrical membrane (Fig. 3B). This indicates that MurJ midcell localization is
243 dependent on the presence of the early divisome. Like in the FtsA(*Ts*) cells, MurJ
244 midcell localization was only observed when grown at permissive conditions, but not
245 at non-permissive conditions in temperature-sensitive strains of the later localizing
246 divisome proteins, FtsQ, FtsW, FtsI (65, 66) or in an FtsN depleted strain (Fig. 3 C-
247 F). These results suggest that MurJ requires a mature divisome for midcell
248 localization. To determine to what extent MurJ is dependent on cell division, we also
249 examined MurJ localization in strains that were deleted for the genes encoding
250 PBP1A, PBP1B, Pal, TolA, or the amidases AmiABC. The observation of a clear
251 MurJ midcell localization in the absence of these proteins, even when cells grow as
252 chains, indicates that MurJ midcell localization is independent of these processes (Fig.
253 3 G-K). All these results support the conclusion that MurJ is specifically recruited to
254 midcell during septal PG synthesis.
255
256 **MurJ midcell localization requires PBP3 activity**. As the putative flippase of lipid
257 II, the next obvious question would be whether the localization of MurJ is dependent
258 on septal PG synthesis. Septal PG synthesis requires the activity of PBP3 (FtsI) and
259 PBP1B, although the latter can be replaced by PBP1A (26). The specific inhibition of
260 PBP3 activity by aztreonam blocks septal PG synthesis without initially inhibiting the
261 localization of the divisome, resulting in filamentous growth of cells with divisomes
262 localized at regular unit cell distances (59, 67). When grown at 28 °C to steady state
263 in Gb1 medium, MurJ localization was determined in the presence of 1 $mg.L^{-1}$
264 aztreonam. Already after 30 min of division inhibition, MurJ midcell localization was
265 lost (Fig. S2), and after 1 MD and 2 MDs, filamentous morphology of cells was

266 observed, and MurJ midcell localization was completely abolished (Fig. S2 and Fig.
267 4). After 2 MDs treatment, cells were fixed and immunolabeled with antibodies
268 against FtsZ and FtsN to show the localization of divisomes, and against MraY and
269 MurG to show the localization of the lipid II-synthesizing complex. As expected, we
270 found that FtsZ, FtsN, MurG and MraY localized at potential division sites in the
271 filaments (Fig. 4). This strongly suggests that MurJ localization is dependent on the
272 activity of PBP3. The midcell localization is specifically dependent on the septal PG
273 synthesis, since MurJ localization was not affected in the presence of elongasome
274 inhibitors A22 and mecillinam for 2 MDs, which inactivate MreB and PBP2,
275 respectively (67–70), although cells started to grow spherical (Fig. S3). Together
276 these results indicate that the lipid II synthesizing proteins MraY and MurG are
277 dependent on the physical presence of the divisome, while the flippase MurJ is not
278 only dependent on the presence of the divisome, but also critically on the activity of
279 septal PG synthesis.
280
281 **MurJ midcell localization requires lipid II synthesis**. As the putative lipid II
282 flippase, we wondered whether MurJ localization would be lipid II-dependent. The
283 biosynthesis of lipid II requires the activity of two essential enzymes in the
284 cytoplasmic stage, the pyridoxal 5'-phosphate (PLP) dependent alanine racemase,
285 Alr, which converts L-alanine into D-alanine (3, 71), and the ATP-dependent D-
286 ala:D-ala ligase, Ddl, which catalyzes the formation of D-alanyl-D-alanine from two
287 molecules D-alanine (3, 72). D-cycloserine (DCS) is a structural analogue of D-
288 alanine that inactivates Alr and Ddl, and causes rapid cell lysis (73–76). At
289 concentration of 1 $\mu g.ml^{-1}$ DCS is sufficient to deplete the lipid I precursor UDP-
290 MurNac-pentapeptide pool in 30 minutes when *E. coli* is grown in Gb1 (77, 78).
291 Therefore, steady-state grown XL08 cells were treated with different concentrations
292 of DCS, and MurJ localization was determined at 30 min, 1 MD and 2 MDs after
293 adding DCS. At concentrations of 0.5 $\mu g.mL^{-1}$ DCS or higher, growth inhibition and
294 rapid cell lysis was observed after 30 min, while lower concentrations of DCS caused
295 lysis after 1 MD or longer (Fig. 5A). Interestingly, DCS also showed a dose-
296 dependent effect on MurJ localization. In 30 min, the increasing DCS concentrations
297 eventually blocked the midcell localization of MurJ, and when the DCS concentration
298 was higher than 0.5 $\mu g.mL^{-1}$, MurJ was mostly absent from midcell (Fig. 5B). In
299 addition, low concentrations of DCS showed a concentration-dependent inhibition on

300 MurJ midcell localization (Fig. S4). Together, these results indicate that MurJ midcell
301 localization is dependent on the synthesis of lipid II.
302
303 **MurJ midcell localization requires FtsW activity**. Our results so far showed that
304 MurJ midcell localization is dependent on the assembly of the divisome, the activity
305 of PBP3 and also the synthesis of lipid II. But because FtsW has been reported to bind
306 lipid II *in vitro* whereas MurJ did not, it could be possible that FtsW was somehow
307 involved in the flipping activity of MurJ. Investigation of divisome assembly and
308 regulation showed that the recruitment of the last divisome protein FtsN to midcell
309 depresses the inactivity of the FtsQLB, which subsequently activates the FtsW-PBP3
310 complex that initiates the synthesis of septal PG (23, 79). Very recently, *in vitro* data
311 showed that FtsW, PBP3 and PBP1B form a ternary complex, and the high lipid II
312 binding affinity of FtsW inhibits the polymerization of lipid II by PBP1B in the
313 absence of PBP3, while the presence of PBP3 stimulates the release of lipid II from
314 FtsW, and activates its polymerization by PBP1B (38). These observations raised the
315 possibility that FtsW is needed to present lipid II to MurJ, which implied that MurJ
316 would not be able to localize at midcell in the presence of inactive FtsW. To validate
317 this hypothesis, plasmids that expressed two non-functional FtsW mutants, FtsW
318 R145A and FtsW K153N were introduced into strain XL08 to investigate the
319 localization of MurJ. These two mutants were shown to localize at midcell but failed
320 to complement the FtsW(*Ts*) strain at non-permissive temperature, and their
321 expression in LMC500 wild-type cells showed a dominant-negative filamentous
322 morphology. In addition, *in vitro* data showed that these mutants lost the lipid II
323 "flipping" activity of FtsW (39). In our study, to eliminate the role of the wild-type
324 FtsW, 20 μM IPTG was used to overexpress these two mutants, and thus diluted the
325 functional copy of FtsW from the XL08 genome. When cells were grown to steady
326 state in minimal medium, cell length increased due to the defect on cell division,
327 especially in cells expressing mutant K153N (Fig. 6B). MurJ midcell localization was
328 lost in the presence of non-functional FtsW mutants for 2 MDs, despite the
329 overexpression of MurJ as it is also expressed under the IPTG inducible $P_{trcdown}$
330 promoter. Whereas the divisome, which was monitored by immunolabeling of FtsN,
331 was still localized at midcell (Fig. 6). Moreover, when grown in LB medium, strains
332 expressing these mutants showed more defects on morphology and MurJ localization.
333 At early exponential phase (OD_{600} = 0.2), filamentous morphology was observed for

334 all cultures, even for cells grown with glucose that suppressed the expression of the
335 FtsW mutants (Fig. S5A). Interestingly, in cultures at late log phase expressing the
336 FtsW K153N mutant or in cultures at stationary phase expressing the FtsW R145A
337 mutant, some cells started to restore the MurJ localization, especially in the cells that
338 were induced with IPTG (Fig. S5A). Since these mutants are toxic, we wondered
339 whether the XL08 strain lost these FtsW expressing plasmids at high frequency,
340 restoring MurJ localization. A spot assay was carried out to test our hypothesis: cells
341 from each culture were diluted to the same OD_{600} value and spotted on LB and LB-
342 ampicillin agar plates (these two mutants plasmids are ampicillin resistant). For both
343 strains, no obvious growth difference was observed on both plates when grown with
344 glucose, indicating that most cells still contained the mutant plasmids. However, for
345 cells that had been induced with IPTG, a large population of cells had lost the FtsW
346 mutant plasmids, as much less growth was observed on the ampicillin plate compared
347 with LB plate (Fig. S5B). These results strongly suggest that MurJ midcell
348 localization requires FtsW activity, rather than its physical presence.
349
350 **MurJ flipping activity is not required for its localization**. Earlier studies revealed
351 several conserved charged residues, R18, R24, R52 and R270 in the central cavity of
352 MurJ that are essential for its function (41–43). To verify whether MurJ needed to be
353 functional to allow midcell localization, an mNG fused MurJ R18A mutant was
354 expressed from plasmid in LMC500. The cells were grown in Gb1 and expression
355 was induced with 20 μM IPTG. As shown in Fig. 7A, the non-functional mutant
356 R18A localized both in the lateral wall and at midcell as was observed for the wild
357 type-MurJ fusion. Although MurJ is likely functional as monomer based on its
358 structure, the wild-type copy of MurJ from LMC500 genome might still contribute to
359 the localization of this non-functional mutant. To eliminate this potential contribution,
360 localization of R18A mutant was also determined in strain XL30, a MurJ-depletion
361 strain in which native MurJ production is under an arabinose-inducible promoter (31).
362 In the presence of arabinose, no growth defect was observed, and the R18A mutant
363 showed the same localization as in the LMC500 strain (Fig. 7B, left). When grown in
364 the presence of glucose, native MurJ was eventually depleted as morphology defects
365 were observed after 3 hours, however, the mutant R18A was still localized in lateral
366 wall and at midcell (Fig. 7B, right). The localization of the other loss-of-function-
367 mutants showed the same results as R18A (Fig 9 and Fig. S7). These results suggest

368 that the MurJ function is not required for its localization. Since we showed that MurJ
369 localization is driven by its lipid II substrate, it is likely that these residues are not
370 responsible for the recognition of lipid II, but for flipping lipid II from the central
371 cavity of MurJ.
372
373 **Function and localization of MurJ single-cysteine A29C and S263C variants are**
374 **sensitive to MTSES**. The function of a number of MurJ single-cysteine mutants,
375 A29C, N49C, S263C and E273C, was reported to be sensitive to MTSES (41).
376 MTSES covalently modifies reduced cysteine residues that are exposed to the
377 periplasm. In the absence of MTSES, these mutant proteins are functional, but not
378 when MTSES is bound to their cysteine residues (44, 45, 80). To investigate how
379 MTSES affected the functionality of these mutants, the localization of their mNG
380 fusions was determined in the presence of MTSES. The optimal MTSES
381 concentration was determined to be 0.5 mM for the Gb1 grown strain XL03 that
382 expressed these functional mutants (Material and Methods and Fig. S6). Expression
383 was induced with 20 μM IPTG and 40 μM IPTG to show their functional and
384 localization sensitivities to MTSES, respectively. Surprisingly, MTSES was found to
385 act on these mutants through two different mechanisms, although the function of all
386 these mutants were affected by MTSES as cell lysis was observed after MTSES
387 addition (Fig. 8 A-E). Midcell localization of the mutants A29C and S263C was
388 blocked in the presence of MTSES (Fig. 8 A, B and Fig. S8 B, C). The latter was
389 more sensitive to MTSES as rapid cell lysis was observed in 20 minutes and MurJ
390 localization could only be determined at 10 min and 20 min after MTSES addition. In
391 contrast, the localization of mutants N49C and E273C was not at all affected by
392 MTSES (Fig. 8 C, D and Fig. S8 D, E). Moreover, E273C was reported to be partially
393 functional (42), and indeed morphology defects were observed in many cells, while
394 the MurJ localization was not influenced (Fig. S8E). This supports the notion that
395 MurJ functionality is not essential for its localization. Additionally, the functional
396 cysteine-free mutant (MurJ Cys^-) was not affected by MTSES, neither with respect to
397 growth nor on localization (Fig. 8E). These results indicate that, in the presence of
398 MTSES, the loss of function of mutants A29C and S263C is caused by the loss of
399 their recruitment while for N49C and E273C, only the flipping activity is blocked but
400 not their localization. Recently, a crystal structural study of $MurJ_{TA}$ predicted the
401 existence of the inward- and outward-facing states, and these 4 residues are accessible

402 to MTSES when $MurJ_{TA}$ is in the outward-facing state. Moreover, it was predicted
403 that mutants A29C and S248C (like S263C in *E. coli*) will be trapped in the out-
404 facing state in the presence of MTSES (43). Together, these results strongly suggest
405 that A29 and S263 are involved in the conformational change from outward- to
406 inward-facing state, and when trapped in the outward-facing state by MTSES, MurJ
407 cannot be recruited to midcell anymore. While mutants N49C and E273C are still able
408 to change back into the inward-facing state and localize. Consequently, the inward-
409 facing state is the default state of MurJ, and only in this state, MurJ can be recruited
410 and localized.
411
412 **MTSES does not influence the localization of non-functional MurJ mutants**.
413 Previous research showed that the non-functional MurJ mutants R18C, R24C, R52C,
414 and R270C are also accessible to MTSES (41). And we showed that MurJ
415 functionality is not needed for its localization. To verify whether MTSES influences
416 the localization of these mutants, similar MTSES experiments were performed on
417 these mNG-fused mutants in the LMC500 background. To eliminate the potential
418 influence of MTSES on wild type MurJ from the LMC500 genome, the MurJ deletion
419 strain expressing mNG fused wild-type MurJ was firstly checked. In agreement with
420 the evidence that the two native cysteine residues in wild-type MurJ are not labeled
421 by MTSES, no defect on cell growth, morphology or MurJ localization was observed
422 when MTSES was present (Fig. 8F and Fig. S8F), (41). Similarly, no growth or
423 morphology defect was observed after addition of MTSES to the non-functional
424 single cysteine mutants, and MurJ was still localized at midcell (Fig. 8G, Fig. S7 and
425 Fig. S8 G-K). We should point out that, when induced with 20 μM or 40 μM IPTG,
426 mutant R24C showed strongly reduced fluorescence and a cytoplasmic-like
427 localization, compared to other mutants. However, when induced with 100 μM IPTG,
428 R24C showed a normal MurJ localization and comparable fluorescence, indicating
429 that mutation R24C does not affect MurJ localization (Fig. S7D). Surprisingly, a
430 spontaneous suppressor mutation R447H that is situated at the cytoplasmic end of
431 TMH13 restored fluorescence and showed a typical MurJ localization when induced
432 with 40 μM IPTG (Fig. S7E-G). Since the R24C mutant was reported not to affect
433 protein level (42), R24C might slightly change the structure of MurJ, and affect mNG
434 folding and fluorescence, while mutation R447H could suppress this defect. These
435 results suggest that the non-functional mutants stay in the inward-facing

436 conformation, since we showed that only in this state, MurJ could be recruited to
437 midcell. Furthermore, these results indicate that these mutations cause the loss of
438 MurJ flipping activity, rather than lipid II binding activity, since MurJ midcell
439 localization is substrate dependent.
440
441 **Localization of non-functional double mutant A29C-R52C is not sensitive to**
442 **MTSES**. Our results so far indicate that the inward-facing state is essential for MurJ
443 midcell localization. To verify that the still-localized MTSES treated non-functional
444 mutants (R18C, R24C, R52C, and R270C, and N49C and E273C) are fixed in the
445 inward open conformation, an mNG fused MurJ A29C-R52C double mutant was
446 constructed. The mutant R52C is nonfunctional but still localizes when bound to
447 MTSES, whereas the localization and function of mutant A29C are disrupted by
448 MTSES. The double mutant is expected to be nonfunctional, and if it would be in the
449 inward-facing conformation not able to flip. MTSES is expected not to affect its
450 localization because residue A29C is not accessible in this state. Indeed, the double
451 mutant failed to complement MurJ depletion indicating the loss of MurJ function.
452 Interestingly, in contrast with single mutant A29C but like the non-functional single
453 mutant R52C, this double mutant showed clear midcell localization in the presence of
454 MTSES (Fig. 8H). Apparently R52C prevented the accessibility of A29C to MTSES.
455 This strongly suggests that the localized-loss-of-functional mutants are not able to
456 convert to the outward-facing conformation, and are fixed in the default inward-
457 facing state, which could still be recruited to midcell. More importantly, these results
458 suggest that the flipping of lipid II coincides with its conformational change from
459 inward-facing state into outward-facing state. The subsequent release of lipid II into
460 the periplasm would allow MurJ to switch back to the inward-facing state.
461
462 **Discussion**
463 **Recruitment of MurJ to midcell and the coordination of cell division and septal**
464 **PG synthesis**. The synthesis of PG has been studied for decades, and FtsW and RodA
465 have been always considered as the lipid II flippases in elongasome and divisome,
466 respectively (12, 33, 39, 40, 81–83). Only recently, MurJ was identified as the lipid II
467 flippase (31, 44, 45, 47, 48). FtsW has been shown to bind and flip lipid II and other
468 lipids *in vitro* but not *in vivo* (39, 40), whereas evidence has been provided that MurJ
469 is flipping *in vivo* but not *in vitro* (38, 44, 45). Our study indicates that these

470 observations can be very well all valid, as both FtsW and MurJ are required for lipid
471 II flipping during cell division.
472 Our results show for the first time the specific MurJ cellular localization in *E.*
473 *coli*. Its midcell localization is critically dependent on maturation of the divisome, on
474 PBP3 and FtsW activity, and lipid II synthesis. MurJ can only recognize the substrate
475 and localize to midcell when it is in the inward-facing conformation. In *E. coli*, MurJ
476 can be replaced by non-homologous flippases from other organisms (43, 46–48, 84).
477 Probing the interaction of MurJ with cell division proteins such as PBP3, FtsW, MurG
478 using our cytoplasmic FRET assay (85) did not support interaction between these
479 proteins and MurJ. Although negative FRET results are not at all a guarantee for the
480 absence of interactions, together with the complementation of MurJ by other flippases,
481 it suggests that protein-protein interactions are not involved in MurJ localization,
482 which implies that its localization at midcell is driven by its substrate lipid II. *In vivo*,
483 inactivation of MurJ results in accumulation of lipid II (31, 45), indicating that lipid II
484 synthesis is independent of the flipping process and MurJ's presence is needed for
485 lipid II translocation but not synthesis. Because MurJ midcell localization is driven by
486 the presence of its substrate, the failure of MurJ to localize at an incomplete divisome
487 or upon inactivation of PBP3 (by aztreonam) or FtsW (by mutation) signifies that
488 lipid II is inaccessible to MurJ under these conditions, despite the proper localization
489 of MraY (lipid I production) and MurG (lipid II production) (Fig 3, 4 and 6). But why
490 would lipid II not be accessible to MurJ? FtsW is clearly able to bind lipid II *in vitro*
491 (38), and the absence of PBP3 causes FtsW to hold lipid II and prevents its
492 polymerization by PBP1B, whereas presence of PBP3 stimulates the release of lipid II
493 from FtsW and its polymerization by PBP1B (38). Depletion of RodA and FtsW
494 results in the decrease in levels of PG lipid intermediates (44). Adding that a complete
495 divisome (FtsN arrival) is required to activate the FtsW-PBP3 complex by elevating
496 the repression by FtsQLB (23, 79), a logical explanation would be that Lipid II
497 synthesis at the divisome is stalled in the absence of a functional FtsW. If FtsW would
498 be able to bind and hold Lipid II, it would explain both its lipid II binding *in vitro* and
499 its ability to stall further lipid II synthesis when the divisome is inactivated. Therefore,
500 we propose that FtsW presents lipid II to MurJ, which will ensure that MurJ is only
501 flipping lipid II at the precise position needed.
502
503 Why would it be necessary to present lipid II at midcell to MurJ and does this imply

504 that RodA as an FtsW homolog is also presenting lipid II to MurJ during lateral
505 growth? The midcell position is very precisely determined by the cell (86, 87). If lipid
506 II would be synthesized randomly and flipped randomly, it could lead to loss of
507 precision of the binary fission into identical daughter cells. The observation that
508 inhibition of the elongasome did not affect division or MurJ midcell localization, and
509 the inhibition of the divisome did not influence cell length growth (Fig. 4 and Fig. S3),
510 suggest that lipid II flipping is precisely organized at the position where new PG
511 synthesis should occur. This can be achieved by allowing it only to flip as closely as
512 possible where the substrate is needed, and by only allowing it to bind lipid II next to
513 the proteins that are activated to synthesize the new cell wall.
514
515 **Role of important residues on MurJ function**. MurJ is predicted to cycle between
516 inward-facing and outward-facing conformations (43), and some charged residues
517 were reported to be essential for MurJ function (42), whereas a number of functional
518 cysteine mutants were inactivated by MTSES. Interestingly, most of these residues
519 locate in the central cavity of MurJ (44). But how do these residues contribute to the
520 function and conformation of MurJ? The functional mutants A29C and S263C are not
521 recruited to midcell in the presence of MTSES (Fig. 8 A and B), indicating that they
522 cannot recognize the substrate lipid II anymore. Since these residues are predicted to
523 be accessible in the open-outward conformation (43), binding to MTSES traps MurJ
524 in this conformation, and causes the loss of localization and function of MurJ.
525 Consequently, the inward-facing state is the default structure for MurJ and only in this
526 conformation MurJ can be recruited. This is consistent with the fact that crystalized
527 MurJ showed this conformation (88). However, the other two functional mutants
528 N49C and E273C that are also sensitive to MTSES (Fig. 9 D and E) and the total-
529 loss-of-function mutants R18C, R24C, R52C and R270C are still able to localize at
530 midcell, suggesting that these mutants are in the inward-facing conformation, and
531 therefore are able to recognize substrate but have lost flippase activity. The
532 observation that the MurJ double mutant A29C-R52C is still able to localize at
533 midcell in the presence of MTSES strongly suggests that these loss-of-function
534 mutants stay only in the inward-facing conformation, since A29C is no longer
535 accessible to MTSES, and further indicates that the flipping of lipid II coincides with
536 the MurJ conformational change from inward-facing state into outward-facing state.
537 Narrowing the pore channel by binding MTSES at the non-essential residues N49C

538 and E273C interrupts the passthrough of lipid II during flipping, and traps MurJ in the
539 inward-facing conformation only, which results in the observations that they are
540 originally functional and sensitive to MTSES, but behave like the total-loss-of-
541 function mutants. The conclusion that these identified important residues are
542 responsible for lipid II flipping rather than recognition fits the fact that they are not
543 conserved in the flippases from other bacteria (Fig. S9), which could complement
544 MurJ depletion in *E. coli*. This indicates that Gram negative and Gram positive MurJ
545 might have different flipping mechanisms.
546
547 **Model of MurJ function in septal PG synthesis**. Based on our evidence and that of
548 others (23, 38, 39, 41, 43, 44, 90, 91), we arrived at a model for the mechanism of
549 MurJ recruitment and lipid II flipping during septal PG synthesis (Fig. 9). For MurJ
550 recruitment, the arrival of the last divisome protein FtsN activates the divisome by
551 depressing the inhibition of the FtsQLB complex, and subsequently activating the
552 FtsW-PBP3-PBP1B complex. This promotes the presenting and release of lipid II by
553 FtsW, which recruits MurJ to midcell (Fig. 9 A). This ensures the precise positioning
554 of septal PG synthesis. Interruption of lipid II synthesis by D-cycloserine, or
555 inactivation of PBP3 by aztreonam, or inactivation of FtsW will block lipid II
556 accessibility and MurJ fails to be recruited to midcell. Once recruited, MurJ flips lipid
557 II by changing from the inward-facing state to an outward-facing conformation and
558 presents lipid II for new PG synthesis in the periplasm (Fig. 9 B and C).
559 Subsequently, the unloaded outward facing MurJ switches back to the default inward-
560 facing state, and can be recruited for new cycles (Fig. 9D). Charged residues R18,
561 R24, R52, R270 are essential for the flipping process, and a mutation at these
562 positions, or the binding of MTSES to residues N49C and E273C will trap MurJ in
563 the inward-facing state that is still able to localize (Fig. 9B). While the binding of
564 MTSES on residues A29C and S263C will trap MurJ in the outward-facing state, and
565 prevents it from running new cycles (Fig. 9D). Here, we showed how MurJ flips lipid
566 II during cell division, it should be noted that although we mainly focused on the
567 septal MurJ, some evidence, like the D-cycloserine experiments, MurJ depletion
568 experiment, and MTSES experiments, showed a global effect on *E. coli*, indicating
569 that MurJ very likely works similarly in elongasome, probably with FtsW
570 homologous protein RodA.
571

572 **Materials and Methods**

573 Strains, plasmids and primers used in this study can be found in *SI Appendix, Tables*
574 *S1* and *S2*. Information on strains and plasmids constructing, functionality test,
575 immunolocalization assay, MTSES assay, microscopy and data analysis are described
576 in *SI Materials and Methods*.

577

578

579 **ACKNOWLEDGEMENTS.** We would like to thank Dr. N. Ruiz for critically
580 reading the manuscript and for the gift of plasmids pFLAGMurJΔCys and pRC7MurJ
581 for cloning and the functionality testing.

582 X.L. was supported by the Chinese Scholarship Council (File No.201406220123), and
583 N.Y.M. by NWO ALW open program (822.02.019).

584 X.L. and T.B. designed most experiments. X.L performed most experiments and
585 N.Y.M designed and performed some of the experiments. X.L and TdB analyzed the
586 data and wrote the manuscript. A.B. isolated MraY and made antibodies against the
587 protein. All authors critically read the manuscript and gave feedbacks.

588

589

590

591

592

593

594

595

596

597

598

599

600

601

602

603

604

605

606 ***References***

607 1. Vollmer W, Blanot D, De Pedro MA (2008) Peptidoglycan structure and
608 architecture. *FEMS Microbiol Rev* 32(2):149–167.
609 2. Bouhss A, Trunkfield AE, Bugg TDH, Mengin-Lecreulx D (2008) The
610 biosynthesis of peptidoglycan lipid-linked intermediates. *FEMS Microbiol Rev*
611 32(2):208–233.
612 3. Barreteau H, et al. (2008) Cytoplasmic steps of peptidoglycan biosynthesis.
613 *FEMS Microbiol Rev* 32(2):168–207.
614 4. Pomorski T, Menon AK (2006) Lipid flippases and their biological functions.
615 *Cell Mol Life Sci* 63(24):2908–2921.
616 5. Ruiz N (2016) Filling holes in peptidoglycan biogenesis of *Escherichia coli*.
617 *Curr Opin Microbiol* 34:1–6.
618 6. Ruiz N (2015) Lipid Flippases for Bacterial Peptidoglycan Biosynthesis. *Lipid*
619 *Insights* 8(Suppl 1):21–31.
620 7. Scheffers DJ, Tol MB (2015) LipidII: Just Another Brick in the Wall? *PLoS*
621 *Pathog* 11(12):1–12.
622 8. Macheboeuf P, Contreras-Martel C, Job V, Dideberg O, Dessen A (2006)
623 Penicillin binding proteins: Key players in bacterial cell cycle and drug
624 resistance processes. *FEMS Microbiol Rev* 30(5):673–691.
625 9. Sauvage E, Kerff F, Terrak M, Ayala JA, Charlier P (2008) The penicillin-
626 binding proteins: Structure and role in peptidoglycan biosynthesis. *FEMS*
627 *Microbiol Rev* 32(2):234–258.
628 10. Manat G, et al. (2014) Deciphering the Metabolism of Undecaprenyl-
629 Phosphate: The Bacterial Cell-Wall Unit Carrier at the Membrane Frontier.
630 *Microb Drug Resist* 20(3):199–214.
631 11. Pedro MA De, Quintela JC, Höltje J V, Schwarz H (1997) Murein segregation
632 in *Escherichia coli*. *Microbiology* 179(9):2823–2834.
633 12. Den Blaauwen T, De Pedro MA, Nguyen-Distèche M, Ayala JA (2008)
634 Morphogenesis of rod-shaped sacculi. *FEMS Microbiol Rev* 32(2):321–344.
635 13. van Teeffelen S, et al. (2011) The bacterial actin MreB rotates, and rotation
636 depends on cell-wall assembly. *Proc Natl Acad Sci* 108(38):15822–15827.
637 14. Morgenstein RM, et al. (2015) RodZ links MreB to cell wall synthesis to
638 mediate MreB rotation and robust morphogenesis. *Proc Natl Acad Sci U S A*
639 112(40):12510–12515.
640 15. Fenton AK, Mortaji L El, Lau DTC, Rudner DZ, Bernhardt TG (2016) CozE is
641 a member of the MreCD complex that directs cell elongation in Streptococcus
642 pneumoniae. *Nat Microbiol* 2(December 2016):16237.
643 16. Contreras-Martel C, et al. (2017) Molecular architecture of the PBP2–MreC
644 core bacterial cell wall synthesis complex. *Nat Commun* 8(1):776.
645 17. Sun Q, Margolin W (1998) FtsZ Dynamics during the Division Cycle of Live
646 *Escherichia coli* Cells. 180(8):2050–2056.
647 18. Blaauwen T Den, Buddelmeijer N, Aarsman MEG, Hameete CM, Nanninga N
648 (1999) Timing of FtsZ assembly in *Escherichia coli*. *J Bacteriol* 181(17):5167–
649 5175.
650 19. den Blaauwen T, Hamoen LW, Levin PA (2017) The divisome at 25: the road
651 ahead. *Curr Opin Microbiol* 36:85–94.
652 20. Gray AN, et al. (2015) Coordination of peptidoglycan synthesis and outer
653 membrane constriction during *Escherichia coli* cell division. *Elife* 4(MAY):1–
654 29.
655 21. Aarsman MEG, et al. (2005) Maturation of the *Escherichia coli* divisome

656 occurs in two steps. *Mol Microbiol* 55(6):1631–1645.
657 22. Lutkenhaus J (2009) FtsN - Trigger for septation. *J Bacteriol* 191(24):7381–
658 7382.
659 23. Weiss DS (2015) Last but not least: New insights into how FtsN triggers
660 constriction during *Escherichia coli* cell division. *Mol Microbiol* 95(6):903–
661 909.
662 24. Gerding MA, et al. (2009) Self-enhanced accumulation of FtsN at division sites
663 and roles for other proteins with a SPOR domain (DamX, DedD, and RlpA) in
664 *Escherichia coli* cell constriction. *J Bacteriol* 191(24):7383–7401.
665 25. Bertsche U, et al. (2006) Interaction between two murein (peptidoglycan)
666 synthases, PBP3 and PBP1B, in *Escherichia coli*. *Mol Microbiol* 61(3):675–
667 690.
668 26. Yousif SY, Broome-Smith JK SB (1985) Lysis of *Escherichia coli* by beta-
669 lactam antibiotics: deletion analysis of the role of penicillin-binding proteins
670 1A and 1B. *J Gen Microbiol* 131(10):2839–45.
671 27. Suzuki H, Nishimura Y, Hirota Y (1978) On the process of cellular division in
672 *Escherichia coli*: a series of mutants of *E. coli* altered in the penicillin-binding
673 proteins. *Proc Natl Acad Sci U S A* 75(2):664–668.
674 28. Derouichei R, Bénédetti H, Lazzaroni JC, Lazdunski C, Lloubès R (1995)
675 Protein complex within *Escherichia coli* inner membrane: TolA N-terminal
676 domain interacts with TolQ and TolR proteins. *J Biol Chem* 270(19):11078–
677 11084.
678 29. Dubuisson JF, Vianney A, Lazzaroni JC (2002) Mutational Analysis of the
679 TolA C-Terminal Domain of *Escherichia coli* and Genetic Evidence for an
680 Interaction between TolA and TolB. *J Bacteriol* 184(16):4620–4625.
681 30. Priyadarshini R, De Pedro MA, Young KD (2007) Role of peptidoglycan
682 amidases in the development and morphology of the division septum in
683 *Escherichia coli*. *J Bacteriol* 189(14):5334–5347.
684 31. Ruiz N (2008) Bioinformatics identification of MurJ (MviN) as the
685 peptidoglycan lipid II flippase in *Escherichia coli*. *Proc Natl Acad Sci U S A*
686 105(40):15553–7.
687 32. Young KD (2014) A flipping cell wall ferry. *Microbiology* 345(6193):139–
688 140.
689 33. Ikeda M, et al. (1989) Structural similarity among *Escherichia coli* FtsW and
690 RodA proteins and *Bacillus subtilis* SpoVE protein, which function in cell
691 division, cell elongation, and spore formation, respectively. *J Bacteriol*
692 171(11):6375–6378.
693 34. Meeske AJ, et al. (2016) SEDS proteins are a widespread family of bacterial
694 cell wall polymerases. *Nature* 537(7622):1–15.
695 35. Khattar MM, Begg KJ, Donachie WD (1994) Identification of FtsW and
696 characterization of a new *ftsW* division mutant of *Escherichia coli*. *J Bacteriol*
697 176(23):7140–7147.
698 36. Goehring NW, Gueiros-filho F, Beckwith J (2005) Premature targeting of a cell
699 division protein to midcell allows dissection of divisome assembly in
700 *Escherichia coli*. *Genes Dev* 19(1):127–137.
701 37. Goehring NW, Gonzalez MD, Beckwith J (2006) Premature targeting of cell
702 division proteins to midcell reveals hierarchies of protein interactions involved
703 in divisome assembly. *Mol Microbiol* 61(1):33–45.
704 38. Leclercq S, et al. (2017) Interplay between Penicillin-binding proteins and
705 SEDS proteins promotes bacterial cell wall synthesis. *Sci Rep* 7:43306.

706 39. Mohammadi T, et al. (2014) Specificity of the transport of lipid II by FtsW in
707 *Escherichia coli*. *J Biol Chem* 289(21):14707–14718.
708 40. Mohammadi T, et al. (2011) Identification of FtsW as a transporter of lipid-
709 linked cell wall precursors across the membrane. *EMBO J* 30(8):1425–1432.
710 41. Butler EK, Davis RM, Bari V, Nicholson PA, Ruiz N (2013) Structure-function
711 analysis of MurJ reveals a solvent-exposed cavity containing residues essential
712 for peptidoglycan biogenesis in *Escherichia coli*. *J Bacteriol* 195(20):4639–
713 4649.
714 42. Butler EK, Tan WB, Joseph H, Ruiz N (2014) Charge requirements of lipid II
715 flippase activity in *Escherichia coli*. *J Bacteriol* 196(23):4111–4119.
716 43. Kuk ACY, Mashalidis EH, Lee S-Y (2016) Crystal structure of the MOP
717 flippase MurJ in an inward-facing conformation. *Nat Struct Mol Biol* 24(2):1–
718 8.
719 44. Sham L-T, et al. (2014) MurJ is the flippase of lipid-linked precursors for
720 peptidoglycan biogenesis. *Science (80-)* 345(6193):220–222.
721 45. Qiao Y, et al. (2017) Lipid II overproduction allows direct assay of
722 transpeptidase inhibition by [beta]-lactams. *Nat Chem Biol* 13(7):793–798.
723 46. Ruiz N (2009) *Streptococcus pyogenes* YtgP (Spy-0390) complements
724 *Escherichia coli* strains depleted of the putative peptidoglycan flippase MurJ.
725 *Antimicrob Agents Chemother* 53(8):3604–3605.
726 47. Meeske AJ, et al. (2015) MurJ and a novel lipid II flippase are required for cell
727 wall biogenesis in Bacillus subtilis. *Proc Natl Acad Sci U S A* 112(20):6437–
728 42.
729 48. Elhenawy W, et al. (2016) The o-antigen flippase wzk can substitute for MurJ
730 in peptidoglycan synthesis in helicobacter pylori and *Escherichia coli*. *PLoS*
731 *One* 11(8):1–16.
732 49. van der Ploeg R, Goudelis ST, den Blaauwen T (2015) Validation of FRET
733 Assay for the Screening of Growth Inhibitors of *Escherichia coli* Reveals
734 Elongasome Assembly Dynamics. *Int J Mol Sci* 16(8):17637–54.
735 50. Cranfill PJ, et al. (2016) Quantitative assessment of fluorescent proteins. *Nat*
736 *Methods* 13(7):557–562.
737 51. Meiresonne NY, Ploeg R van der, Hink MA, Tanneke den Blaauwen (2017)
738 Activity-Related Conformational Changes in D,D-Carboxypeptidases Revealed
739 by In Vivo Periplasmic Förster Resonance Energy Transfer Assay in
740 *Escherichia coli*. *MBio* 8(5):e01089-17.
741 52. Chen X, Zaro JL, Shen WC (2013) Fusion protein linkers: Property, design and
742 functionality. *Adv Drug Deliv Rev* 65(10):1357–1369.
743 53. Li GW, Burkhardt D, Gross C, Weissman JS (2014) Quantifying absolute
744 protein synthesis rates reveals principles underlying allocation of cellular
745 resources. *Cell* 157(3):624–635.
746 54. Vischer NOE, et al. (2015) Cell age dependent concentration of *Escherichia*
747 *coli* divisome proteins analyzed with ImageJ and ObjectJ. *Front Microbiol*
748 6(JUN):1–18.
749 55. Huang Y (2003) Structure and Mechanism of the Glycerol-3-Phosphate
750 Transporter from *Escherichia coli*. *Science (80-)* 301(5633):616–620.
751 56. Oswald F, Varadarajan A, Lill H, Peterman EJG, Bollen YJM (2016) MreB-
752 Dependent Organization of the E. coli Cytoplasmic Membrane Controls
753 Membrane Protein Diffusion. *Biophys J* 110(5):1139–1149.
754 57. Mengin-Lecreulx D, Texier L, Rousseau M, Van Heijenoort J (1991) The
755 murG gene of *Escherichia coli* codes for the UDP-N-acetylglucosamine:N-

acetylmuramyl-(pentapeptide) pyrophosphoryl-undecaprenol N-acetylglucosamine transferase involved in the membrane steps of peptidoglycan synthesis. *J Bacteriol* 173(15):4625–4636.

58. Bouhss A, Mengin-Lecreulx D, Le Beller D, Van Heijenoort J (1999) Topological analysis of the MraY protein catalysing the first membrane step of peptidoglycan synthesis. *Mol Microbiol* 34(3):576–585.

59. Mohammadi T, et al. (2007) The essential peptidoglycan glycosyltransferase MurG forms a complex with proteins involved in lateral envelope growth as well as with proteins involved in cell division in *Escherichia coli*. *Mol Microbiol* 65(4):1106–1121.

60. Bisson Filho AW, et al. (2016) Treadmilling by FtsZ filaments drives peptidoglycan synthesis and bacterial cell division. *bioRxiv*. doi:10.1101/077560.

61. Buddelmeijer N, Aarsman M, Blaauwen T den (2013) Immunolabeling of Proteins in situ in *Escherichia coli* K12 Strains. *Bio-Protocol* 3(15):1–5.

62. Pichoff S, Lutkenhaus J (2005) Tethering the Z ring to the membrane through a conserved membrane targeting sequence in FtsA. *Mol Microbiol* 55(6):1722–1734.

63. Rico AI, García-Ovalle M, Mingorance J, Vicente M (2004) Role of two essential domains of *Escherichia coli* FtsA in localization and progression of the division ring. *Mol Microbiol* 53(5):1359–1371.

64. Pichoff S, Lutkenhaus J (2002) Unique and overlapping roles for ZipA and FtsA in septal ring assembly in *Escherichia coli*. *EMBO J* 21(4):685–693.

65. Taschner PE, Huls PG, Pas E, Woldringh CL (1988) Division behavior and shape changes in isogenic *ftsZ*, *ftsQ*, *ftsA*, *pbpB*, and *ftsE* cell division mutants of *Escherichia coli* during temperature shift experiments. *J Bacteriol* 170(4):1533–1540.

66. Ishino F, et al. (1989) New mutations *fts-36*, *lts-33*, and *ftsW* clustered in the mra region of the *Escherichia coli* chromosome induce thermosensitive cell growth and division. *J Bacteriol* 171(10):5523–5530.

67. Den Blaauwen T, Aarsman MEG, Vischer NOE, Nanninga N (2003) Penicillin-binding protein PBP2 of *Escherichia coli* localizes preferentially in the lateral wall and at mid-cell in comparison with the old cell pole. *Mol Microbiol* 47(2):539–547.

68. White CL, Gober JW (2012) MreB: Pilot or passenger of cell wall synthesis? *Trends Microbiol* 20(2):74–79.

69. Vollmer W, et al. (2005) Structural and mechanistic basis of penicillin-binding protein inhibition by lactivicins. *FEMS Microbiol Rev* 30(2):565–569.

70. Shih YL, Kawagishi I, Rothfield L (2005) The MreB and Min cytoskeletal-like systems play independent roles in prokaryotic polar differentiation. *Mol Microbiol* 58(4):917–928.

71. Wood BWA, Gunsalusa IC (1959) D-Alanine formation; a racemase in *Streptococcus faecalis*. *J Biol Chem* 190:403–416.

72. Neuhaus FC (1962) The enzymatic synthesis of D-alanyl-D-alanine. I. Purification and properties of D-alanyl-D-alanine synthetase. *J Biol Chem* 237(3).

73. Wang E, Walsh C, Walsh C (1978) Suicide substrates for the alanine racemase of *Escherichia coli*. *Biochemistry* 17(7):1313–1321.

74. Neuhaus FC, Lynch JL (1972) Studies on the inhibition of D-alanyl-D-alanine synthetase by the antibiotic D-cycloserine. *Biochem Biophys Res Commun*

806 8(5):377–382.
807 75. Azam MA, Jayaram U (2015) Inhibitors of alanine racemase enzyme: a review.
808 *J Enzyme Inhib Med Chem* 6366(August):1–10.
809 76. Prosser G a, de Carvalho LPS (2013) Kinetic mechanism and inhibition of
810 *Mycobacterium tuberculosis* D-alanine:D-alanine ligase by the antibiotic D-
811 cycloserine. *FEBS J* 280(4):1150–66.
812 77. de Roubin MR, Mengin-Lecreulx D, van Heijenoort J (1992) Peptidoglycan
813 biosynthesis in *Escherichia coli*: variations in the metabolism of alanine and D-
814 alanyl-D-alanine. *J Gen Microbiol* 138 Pt 8(1 992):1751–7.
815 78. Mengin-lecreulx D, et al. (1983) Pool Levels of UDP N-Acetylglucosamine
816 and UDP N- Acetylglucosamine-Enolpyruvate in *Escherichia coli* and
817 Correlation with Peptidoglycan Synthesis. 154(3):1284–1290.
818 79. Liu B, Persons L, Lee L, de Boer PAJ (2015) Roles for both FtsA and the
819 FtsBLQ subcomplex in FtsN-stimulated cell constriction in *Escherichia coli*.
820 *Mol Microbiol* 95(6):945–970.
821 80. Chamakura KR, et al. (2017) A viral protein antibiotic inhibits lipid II flippase
822 activity. *Nat Microbiol*. doi:10.1038/s41564-017-0023-4.
823 81. Matsuzawa H, Hayakawa K, Sato T, Imahori K (1973) Characterization and
824 genetic analysis of a mutant of *Escherichia coli* K-12 with rounded
825 morphology. *J Bacteriol* 115(1):436–442.
826 82. Sieger B, Schubert K, Donovan C, Bramkamp M (2013) The lipid II flippase
827 RodA determines morphology and growth in *Corynebacterium glutamicum*.
828 *Mol Microbiol* 90(5):966–982.
829 83. Dai K, Lutkenhaus J (1991) *ftsZ* is an essential cell division gene in
830 *Escherichia coli*. *J Bacteriol* 173(11):3500–3506.
831 84. Fay A, Dworkin J (2009) *Bacillus subtilis* homologs of MviN (MurJ), the
832 putative *Escherichia coli* lipid II flippase, are not essential for growth. *J*
833 *Bacteriol* 191(19):6020–6028.
834 85. Alexeeva S, Gadella TWJ, Verheul J, Verhoeven GS, Den Blaauwen T (2010)
835 Direct interactions of early and late assembling division proteins in *Escherichia*
836 *coli* cells resolved by FRET. *Mol Microbiol* 77(2):384–398.
837 86. Rowlett VW, Margolin W (2015) The Min system and other nucleoid-
838 independent regulators of Z ring positioning. *Front Microbiol* 6(MAY):1–10.
839 87. Ortiz C, Natale P, Cueto L, Vicente M (2015) The keepers of the ring:
840 Regulators of FtsZ assembly. *FEMS Microbiol Rev* 40(1):57–67.
841 88. Pastoret S, et al. (2004) Functional Analysis of the Cell Division Protein FtsW
842 of *Escherichia coli*. *J Bacteriol* 186(24):8370–8379.
843 89. Tsang MJ, Bernhardt TG (2015) Guiding divisome assembly and controlling its
844 activity. *Curr Opin Microbiol* 24:60–65.
845 90. Du S, Pichoff S, Lutkenhaus J (2016) FtsEX acts on FtsA to regulate divisome
846 assembly and activity. *Proc Natl Acad Sci*:201606656.
847
848
849
850
851
852

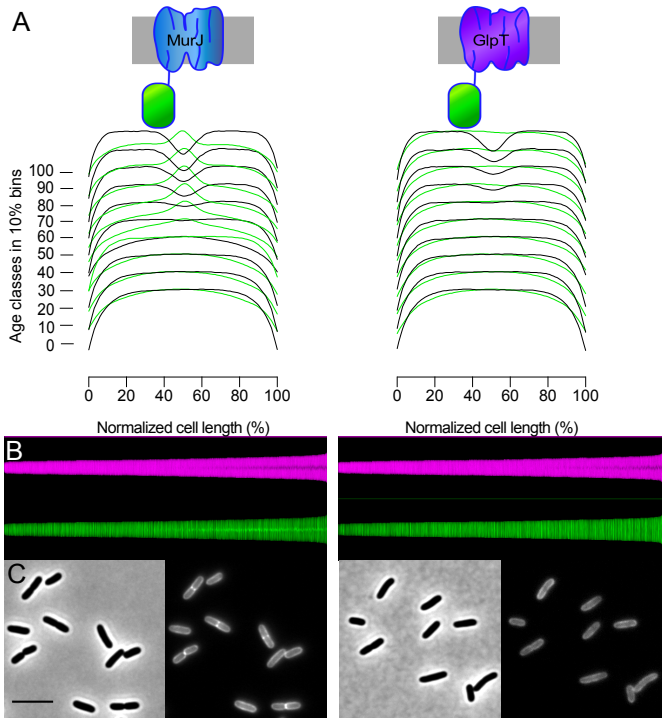

Fig. 1. MurJ localizes both in the lateral wall and at midcell. Strain XL08 containing the chromosomal mNG-MurJ fusion shows a cell-cycle-dependent localization in contrast to the homogenously localizing integral membrane protein mNG-GlpT. Cells were grown in Gb1 minimal medium to steady state at 28°C. Left: MurJ profiles; Right: membrane control protein GlpT profiles. (A) For each protein, the diameter (black lines) and fluorescence (green lines) profiles along normalized cell length are shown in 10 % age class bins. (B) Maps of diameter profiles (magenta) and fluorescence profiles (green). Cells are plotted by length, ascending from left to right. (C) Phase contrast image (left) and the corresponding fluorescence image (right) for each protein. Scale bar equals 5 µm. At least 1200 cells were included for both analyses.

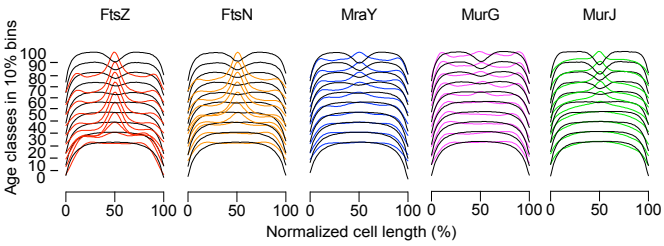

Fig. 2. Timing of MurJ midcell localization. mNG-$(GGS)_2$-MurJ cellular localization was compared with the localization of divisomal and PG precursor synthesizing proteins. XL08 strain was grown to steady state in Gb1 medium. MurJ localization was determined in living cells. After fixation with FAGA, the rest of cells were immunolabeled with antibodies against FtsZ, FtsN, MraY and MurG. Diameter (black lines) and Fluorescence (colored lines) profiles were plotted into 10 % age class bins along the normalized cell length in %. At least 1200 cells were included.

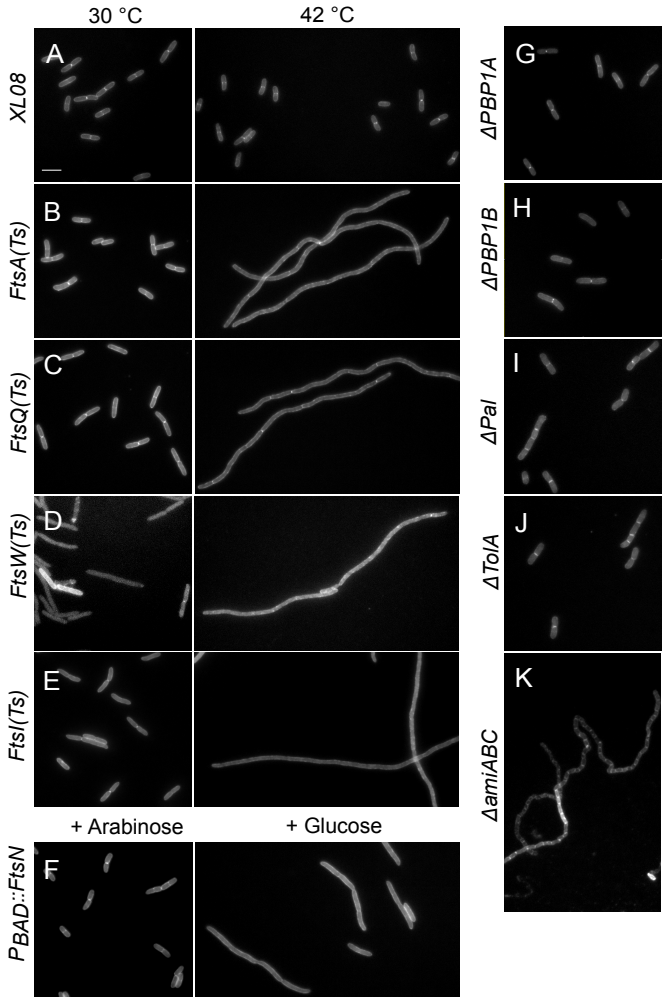

Fig. 3. MurJ requires the core divisome for its midcell localization. Chromosomal mNG-$(GGS)_2$-MurJ fusion was introduced into strains that harbor temperature sensitive, depletable, or deleted division proteins (except that the mNG-$(GGS)_2$-MurJ plasmid was expressed in *ΔtolA and Δpal strains, and the* mCherry-MurJ plasmid was expressed in *ΔamiABC* strain). (A-E) MurJ localization in XL08 (WT), *ftsA 1882* (Ts), *ftsQ1* (Ts), *ftsW* (Ts) and *ftsI2185* (Ts) backgrounds. Left: Localization at permissive temperature of 28 °C. Right: Localization after growth at the non-permissive temperature of 42 °C for 2 mass doublings (MD)s. (F) MurJ localization in FtsN depletion background at 30 °C. Left: localization in the presence of 0.2% w/v arabinose. Right: Localization of MurJ in the absence of arabinose for 2 MDs. (G-H) mCh-MurJ localization in *ΔmrcA* (PBP1A), *ΔmrcB* (PBP1B), *Δpal, ΔtolA* and *ΔamiABC* background at 30 °C, respectively. Scale bar equals 5 μm.

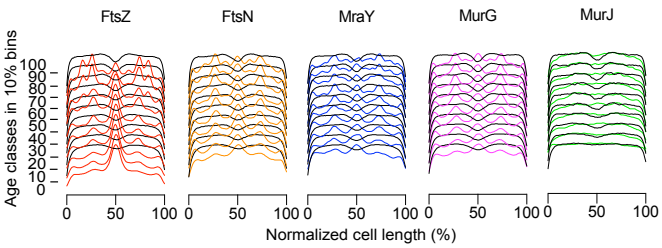

Fig. 4. Localization of cell division proteins in the presence of the PBP3 inhibitor aztreonam for 2 MDs. Cell division is inhibited but the localization and assemblage of the divisome continues, whereas the localization of MurJ is lost. In Gb1 at 28 °C, steady state growing XL08 was treated with 1 mg.L^{-1} aztreonam, MurJ localization was determined in living cells, and FtsZ, FtsN, MraY and MurG were immunolabeled with antibodies after fixation. Diameter (black lines) and fluorescence (colored lines) profiles were plotted into 10 % age class bins along the normalized cell length. At least 1200 cells were included.

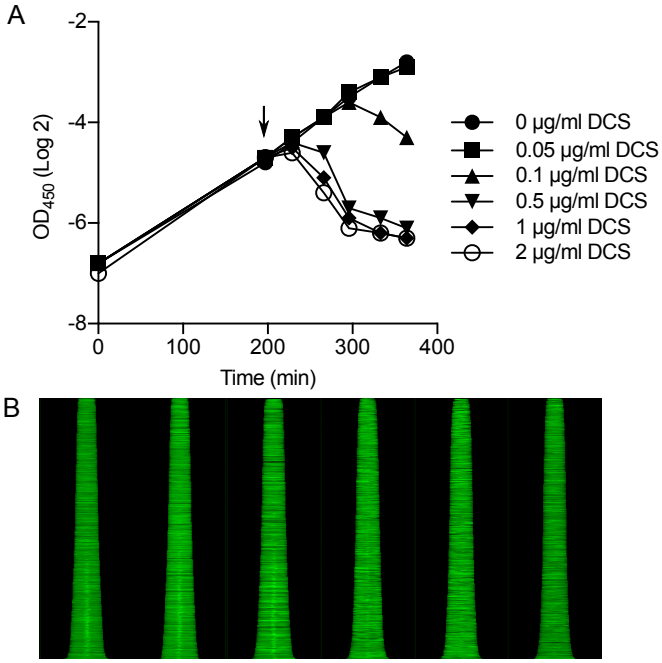

Fig. 5 Inhibition of lipid II biogenesis blocks MurJ midcell localization. In Gb1 at 28 °C, steady state growing XL08 was treated with increasing concentrations of D-cycloserine (DCS), and mNG-MurJ localization was determined at 30 minutes after addition of DCS. (A) Growth curves were plotted as time against the natural logarithm of the optical density of the cells. The black arrow indicates the addition of DCS. (B) Fluorescence maps of MurJ localization. Cells are plotted according to increasing cell length from top to bottom. From left to right, the maps correspondent to 0, 0.05, 0.1, 0.5, 1 and 2 µg.L^{-1} DCS. At least 1200 cells were included.

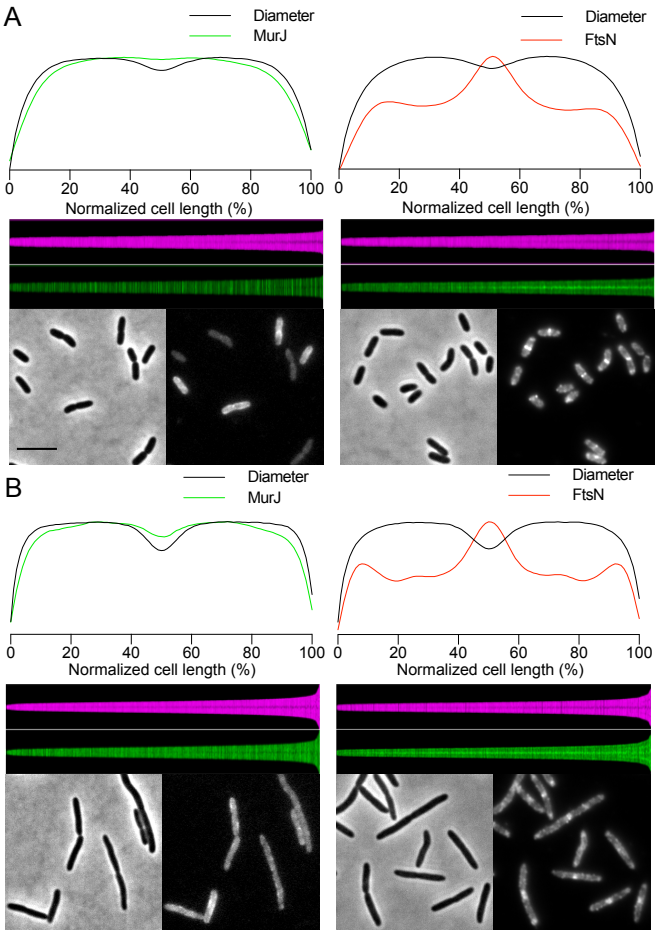

Fig. 6. Non-functional FtsW mutants R145A (A) and K153N (B) abolish MurJ midcell localization. XL08 expressing mutant FtsW R145A or FtsW K153N was grown in Gb1 minimal medium to steady state at 28 °C. IPTG (20 μM) was used to induce expression of the FtsW mutants from plasmid. MurJ localization was determined in living cells and the presence of the divisome was confirmed by immunolabeling of FtsN, after fixation. Top, average localization profiles plotted along normalized cell length (n ≥1200 cells). Black lines indicate cell diameter. Green lines and red lines indicate MurJ and FtsN localization, respectively. Middle, map of profiles of cell diameter and MurJ or FtsN localization sorted by ascending cell length. Bottom, phase contrast and fluorescence microscopy images. Scale bar equals 5 μm.

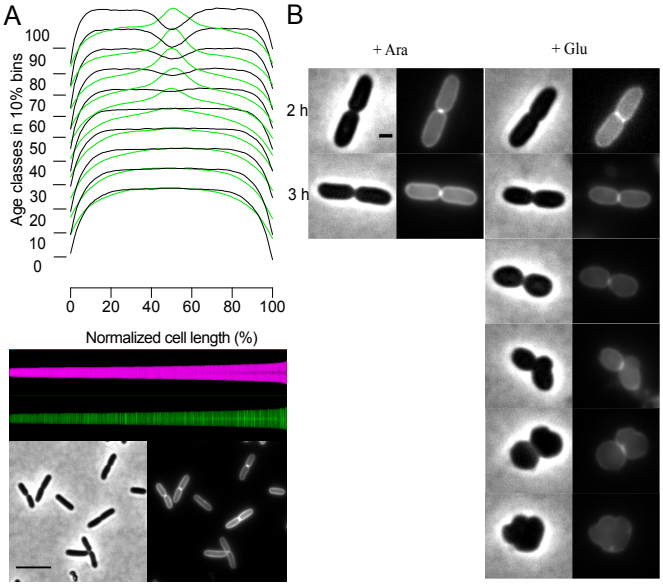

Fig. 7. MurJ non-functional mutant R18A does not influence its localization. (A) The plasmid expressing the mNG-MurJ R18A fusion was introduced into LMC500. This strain was grown in Gb1 minimal medium to steady state at 28 °C, and expression was induced with 20 μM IPTG for 2 MDs. Localization was determined and presented as outlined in Fig 1. At least 1200 cells were included. Scale bar equals 5 μm. (B) The plasmid expressing the mNG-MurJ R18A fusion was introduced into the MurJ depletion strain XL20. Mutant localization was determined in the presence of arabinose (wild type MurJ expression) or glucose (wild type MurJ depletion). Scale bar equals 1 μm.

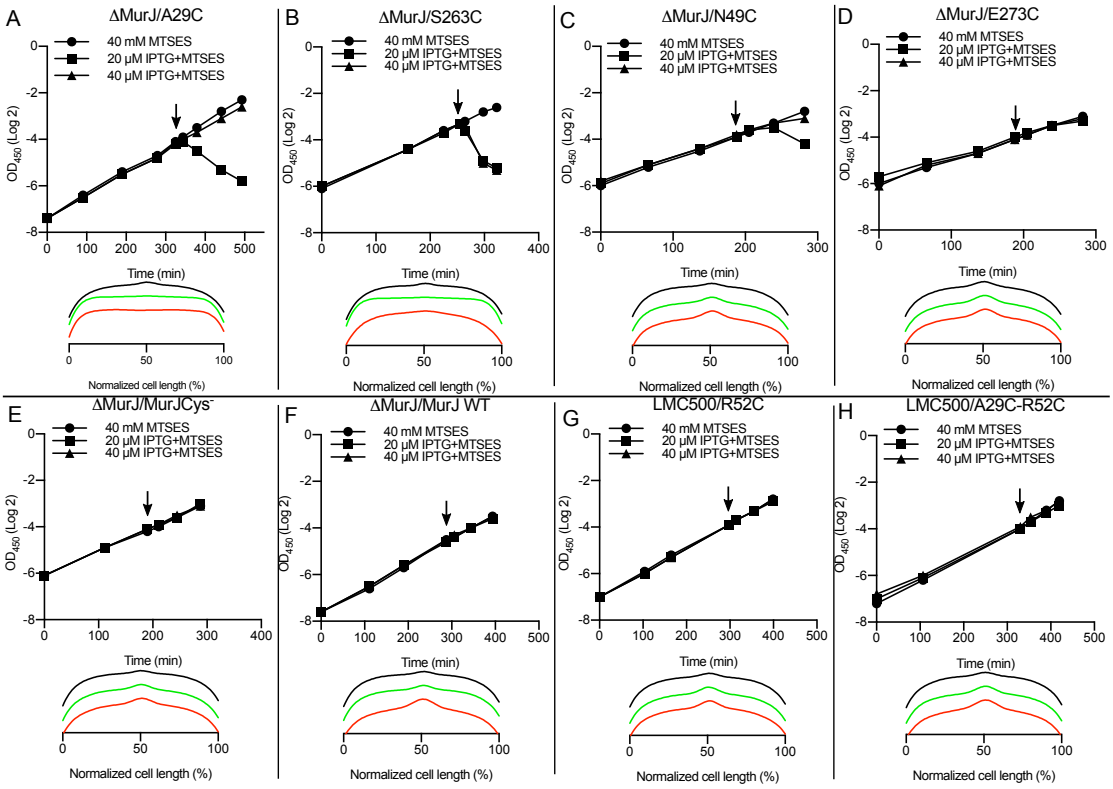

Fig. 8. MurJ mutants behave differently in the presence of MTSES. Strains expressing MurJ single-cysteine-mutants from plasmid were grown to steady state in Gb1 medium at 28 °C, and expression was induced with IPTG for 2 MDs. MurJ localization was determined at 10 minutes and 40 minutes after the addition of MTSES (for mutant S263C, localization was determined at 10 minutes and 20 minutes since it is more sensitive to MTSES), Average of MurJ localization profiles were plotted along normalized cell axis. Black lines indicate the MurJ localization in the absence of MTSES, green and red lines indicate the MurJ localization at 10 and 40 min in the presence of MTSES, respectively. (A and B) Growth and localization of functional mutants A29C and S263C are affected by MTSES. (C and D) Only growth but not localization of functional mutants N49C and E273C are affected by MTSES. (E) Growth and localization of cysteine free mutants are not altered by MTSES. (F) Growth and localization of wild type MurJ are not changed by MTSES. (G) Localization of non-functional MurJ mutant R52C is not affected by MTSES. (H) Localization of non-functional MurJ double mutant A29C-R52C is not influenced by MTSES.

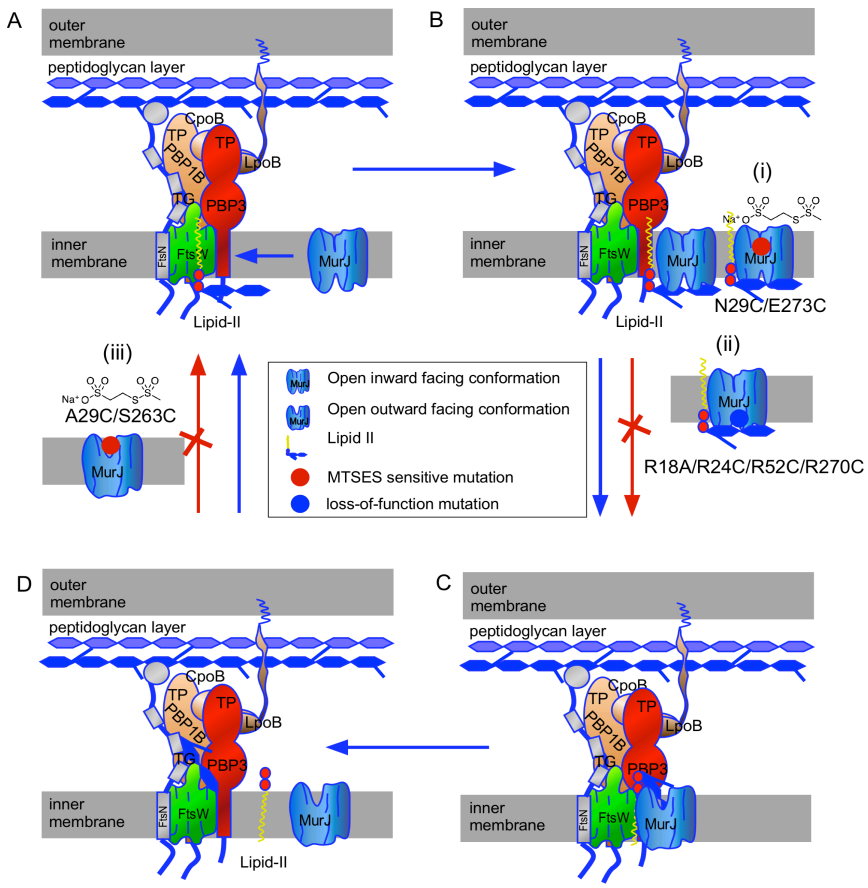

Figure 9. Model of MurJ recruitment and function in septal peptidoglycan synthesis. (A) Recruitment of MurJ to midcell when FtsW is activated. (B) Presenting of lipid II from FtsW to MurJ. (C) MurJ flips lipid II across the IM by changing its conformation structure from the inward-facing state into outward-facing state. (D) Unloaded MurJ changes back into default inward-facing state to participate in the new cycle. (i) Functional MurJ mutants that are inactivated by MTSES still localize but are not able to change from inward-facing conformation into outward-facing conformation. (ii) Loss-of-function MurJ mutants that localize but are not able to change from inward-facing conformation into outward-facing conformation. (iii) Functional MurJ mutants that are fixed in the outward open conformation upon binding of MTSES.

Table 1. Functionality and localization of MurJ fluorescence proteins fusions with different linkers at N- or C- terminus

Fusions	Plasmids	Complementation[a]	Localization[b]	Function[c]
No fusion	pTHV037-MurJ	≈16h	ND	+
	pSAV057-MurJ	≈16h	ND	+
N-terminus	pTHV037-mCh-$(GGS)_n$-MurJ	≈16h	+	+
	pSAV057-mNG-$(GGS)_n$-MurJ	≈16h	+	+
	pSAV057-mKO-MurJ	≈16h	+	+
C-terminus	pTHV037-MurJ-$(GGS)_n$-mCh	≥3 days	−	−
	pSAV057-MurJ-$(GGS)_n$-mNG	≥3 days	−	−

n: Number of GGS repeats (n = 0, 1, 2, 3)

[a] after transformation, the time period needed for visible white colony appearance.

[b] +, FP fused MurJ is fluorescent and localizes in the membrane; −, FP fused MurJ is fluorescent and localizes in the cytosol.

[c] +, functional fusion; −, loss-of-function fusion.